Advances in Difference Equations
a SpringerOpen Journal

RESEARCH   **Open Access**

Stoichiometric knife-edge model on discrete time scale

Ming Chen[1*] ![ORCID], Lale Asik[2] and Angela Peace[2]

*Correspondence:
chenm688@dlmu.edu.cn
[1] School of Science, Dalian Maritime
University, Dalian, China
Full list of author information is
available at the end of the article

Abstract

Ecological stoichiometry is the study of the balance of multiple elements in ecological interactions and processes (Sterner and Elser in Ecological Stoichiometry: The Biology of Elements from Molecules to the Biosphere, 2002). Modeling under this framework enables us to investigate the effect nutrient content on organisms whether the imbalance involves insufficient or excess nutrient content. This phenomenon is called the "stoichiometric knife-edge". In this paper, a discrete-time predator–prey model that captures this phenomenon is established and qualitatively analyzed. We systematically expound the similarities and differences between our discrete model and the corresponding continuous analog. Theoretical and numerical analyses show that while the discrete and continuous models share many properties, differences also exist. Under certain parameter sets, the models exhibit qualitatively different dynamics. While the continuous model shows limit cycle, Hopf bifurcation, and saddle-node bifurcation, the discrete-time model exhibits richer dynamical behaviors, such as chaos. By comparing the dynamics of the continuous and discrete model, we can conclude that stoichiometric effects of low food quality on predators are robust to the discretization of time. This study can possibly serve as an example for pointing to the importance of time scale in ecological modeling.

Keywords: Ecological stoichiometry; Discrete model; Stoichiometric knife-edge; P:C ratio

1 Introduction

Ecological stoichiometry is the study of the balance of energy and essential chemical elements throughout ecological systems [23]. The ratios of elements, such as carbon (C) and phosphorus (P), vary within and across trophic levels and play important roles in ecological interactions. Stoichiometric population models have been widely used to understand predator–prey dynamics under nutritional constraints [3, 10, 20, 21, 27]. Loladze et al. 2000 [17] formulated a tractable two-dimensional Lotka–Volterra type model (LKE model) that incorporates the transfer of elements between predator and prey, where the prey is a primary producer and the predator is a grazer. During the last decades, the LKE model has been extended in the study of plant–herbivore interactions [15], competition among consumers [18], three trophic level food chain [6, 19], seasonal variation in the carrying capacity [2]. All these stoichiometric models show that low nutrient food content (low P:C ratio) causes a nutrient deficiency in grazers.

Springer

It is well known that the selection of time scale is very important in biological and ecological studies [13]. The above-mentioned stoichiometric models are continuous in time. The sensitivity of stoichiometric effects to time discretization has been the subject of recent studies. Fan *et al.* [12], Sui *et al.* [24], Xie *et al.* [28], and Chen *et al.* [7] compared the continuous stoichiometric LKE producer–grazer model [17], a stoichiometric plant–herbivore model [15], a model with one-prey and two-predators [18], and a tritrophic food chain model [19] to their discrete analogs, respectively.

Through numerical and bifurcation analyses these studies investigated the dynamic behaviors of the discrete models, compared them with their corresponding continuous models. Many similarities were found between the dynamics of the continuous models and their discrete analogs. However, different from the corresponding time-continuous models, the time-discrete models exhibit new phenomena, such as chaos.

Recent discoveries in ecological stoichiometry suggest that grazer dynamics are not only affected by insufficient food nutrient content but also by excess food nutrient content (high P:C ratio). This phenomenon is known as the "stoichiometric knife edge" [4, 11]. Elser 2012 [10] and Peace 2013 [21] proposed a stoichiometric model in order to investigate the growth response of grazer to producer of varying P:C ratios capturing the mechanism of the knife-edge phenomenon. These stoichiometric models are defined on the continuous time scale; however, empirical data in ecological systems are collected on discrete time intervals. Indeed many plants in natural and agricultural settings have non-overlapping generations, and many herbivores exhibit annual or seasonal dynamics [28].

The effects of the knife-edge phenomenon can significantly impact population dynamics when environmental nutrient loads are high. It is important to investigate how sensitive these effects are to time discretization. The objective of the work presented here is to compare the dynamics of the continuous stoichiometric knife-edge model [21] with its discrete analog. In particular, we focus on whether the discrete model can retain the most important dynamical features exhibited in the continuous stoichiometric knife-edge model, like deterministic extinction of grazer when faced with excess food-nutrient content (i.e., low food quality). Also, we concentrate on whether chaotic dynamics can arise in the discrete model when the parameters are the same as the continuous one. In the next section, a discrete analog of the producer-grazer model with the effect of the stoichiometric knife-edge is conducted. In Sects. 2 and 3, we explore the dynamics of the discrete model qualitatively. Comparison between our discrete model and its continuous analog by numerical simulations can be found in Sect. 5. In the discussion, we address the implications of our findings.

2 Model construction

Using stoichiometric principles, Peace 2013 [21] proposed a two-trophic-level model that takes the following form:

$$
\begin{aligned}
\frac{dx}{dt} &= bx\left(1 - \frac{x}{\min\{K, (P_T - \theta y)/q\}}\right) - \min\left\{f(x), \frac{\hat{f}\theta}{Q}\right\}y, \\
\frac{dy}{dt} &= \min\left\{\hat{e}f(x), \frac{Q}{\theta}f(x), \hat{e}\hat{f}\frac{\theta}{Q}\right\}y - dy,
\end{aligned}
\tag{2.1}
$$

where $Q = (P_T - \theta y)/x$ describes the variable P quota of the producer. Here $x(t)$ is the density of producer (in milligrams of carbon per liter, mg C/L), $y(t)$ is the density of grazer

(mg C/L), b is the maximum growth rate of producer (day^{-1}), d is the specific loss rate of grazer that includes metabolic losses (respiration) and death (day^{-1}), $\hat{e}$ is the maximum production efficiency of the grazer (no unit) and the second law of thermodynamics requires that $\hat{e} < 1$, K is the producer's *constant* carrying capacity based on light intensity, and $f(x)$ is the grazer's ingestion rate (day^{-1}), which is taken here as a Holling type-II functional response. In general, the function $f(x)$ is a bounded differentiable function that satisfies $f(0) = 0$, $f'(x) > 0$, $f'(0) < \infty$, and $f''(x) < 0$ for $x \geq 0$ [17]. $f(x)$ is saturating with $\lim_{x \to \infty} f(x) = \hat{f}$. The model makes the following four assumptions:

A1: *The total mass of phosphorus in the entire system is fixed, i.e., the system is closed for phosphorus with a total of P_T (mg P/L).*

A2: P:C ratio *in the producer varies, but never falls below a minimum q (mg P/mg C); the grazer maintains a constant P:C, θ (mg P/mg C).*

A3: *All phosphorus in the system is divided into two pools:* P *in the grazer and* P *in the producer.*

A4: *The grazer ingests* P *up to the rate required for its maximal growth but not more.*

These assumptions introduce new constraints in terms of P and C. Three minimum functions have been obtained according to Liebig's law of the minimum. Here, the first minimum function $\min\{K, (P_T - \theta y)/q\}$ is used to describe the producer carrying capacity determined by C (light) and P availability. The second minimum function $\min\{f(x), \hat{f}\theta/Q\}$ is used to describe the grazer ingestion rate. The first input $f(x)$ is the grazer ingestion rate when P is not excess, and the second input $\hat{f}\theta/Q$ is the ingestion rate of grazer when P is in excess. The third minimum function $\min\{\hat{e}f(x), Qf(x)/\theta, \hat{e}\hat{f}\theta/Q\}$ is used to describe the grazer's biomass growth rate, determined by energy limitation, P limitation, and P in excess.

Now we consider the discrete analogue of the above continuous stoichiometric knife-edge model (2.1). There are several methods for discretization of the continuous-time models known to theoretical ecologists [14, 25]. We discretize the model (2.1) applying the method developed by Cook, Busenberg, Wiener, and Shah [5, 8] and used in many papers [7, 12, 16, 22, 24, 28]. This method employs the differential equations with piecewise constant arguments (EPCA) by assuming that on a given time interval $[t, t + 1]$ the per capita growth rate stays constant.

First, we assume that the per capita growth rates in equation (2.1) change only at the time of each measurement. Incorporating this aspect in equation (2.1) yields the following modified system:

$$\frac{1}{x(t)}\frac{dx(t)}{dt} = b\left(1 - \frac{x[t]}{\min(K, (P_T - \theta y[t])/q)}\right) - \min\left\{\frac{f(x[t])}{x[t]}, \frac{\hat{f}\theta}{P_T - \theta y([t])}\right\}y([t]),$$

$$\frac{1}{y(t)}\frac{dy(t)}{dt} = \min\left\{\hat{e}f(x[t]), \frac{P_T - \theta y[t]}{\theta}\frac{f(x[t])}{x[t]}, \frac{\hat{e}\hat{f}\theta x[t]}{P_T - \theta y[t]}\right\} - d, \quad t \neq 0, 1, 2, \ldots, \tag{2.2}$$

where $[t]$ denotes the integer part of $t \in (0, +\infty)$. By a solution of system (2.2), we mean a function $S = (x, y)^T$ which is defined for $t \in [0, \infty)$ and possesses the following properties:

1 S is continuous on $[0, \infty)$.

2 The derivatives $\frac{dx(t)}{dt}$ and $\frac{dy(t)}{dt}$ exist at each point $t \in [0, \infty)$ with the possible exception of the points $t \in \{0, 1, 2, \ldots\}$, where left-sided derivatives exist.

3 System (2.2) is valid on each interval $[n, n + 1)$ with $n = 0, 1, 2, \ldots$.

Table 1 Parameters of model (2.4) with default values

Parameter		Value	Unit
P_T	Total phosphorus	0–0.14	mg P/L
$\hat{e}$	Maximal production efficiency of the grazer	0.8	–
b	Maximal growth rate of the producer	1.2	/day
d	Grazer loss rate (include respiration)	0.25	/day
θ	Grazer constant P:C	0.03	mg P/mg C
q	Producer minimal P:C	0.0038	mg P/mg C
c	Maximal ingestion rate of the grazer	0.81	/day
a	Half-saturation of the grazer ingestion response	0.25	mg C/L
K	Producer carrying capacity limited by light	1.5	mg C/L

Next we integrate both sides of equation (2.2) on any interval of the form $[n, n + 1)$, $n = 0, 1, 2, \ldots$, and obtain, for $n \le t < n + 1$, $n = 0, 1, 2, \ldots$,

$$
\begin{aligned}
x(t) = x(n) \exp\Bigg\{ & \Bigg[b - \frac{bx(n)}{\min\{K, (P_T - \theta y(n))/q\}} \\
& - \min\Bigg\{ \frac{f(x(n))}{x(n)}, \frac{\hat{f}\theta}{P_T - \theta y(n)} \Bigg\} y(n) \Bigg] (t - n) \Bigg\},
\end{aligned}
\tag{2.3}
$$

$$
y(t) = y(n) \exp\Bigg\{ \Bigg[\min\Bigg\{ \hat{e}f(x(n)), \frac{P_T - \theta y(n)}{\theta} \frac{f(x(n))}{x(n)}, \frac{\hat{e}\hat{f}\theta x(n)}{P_T - \theta y(n)} \Bigg\} - d \Bigg] (t - n) \Bigg\}.
$$

Letting $t \to n + 1$, we obtain the following discrete-time analog of system (2.1):

$$
\begin{aligned}
x(n + 1) = x(n) \exp\Bigg\{ & b - \frac{bx(n)}{\min\{K, (P_T - \theta y(n))/q\}} \\
& - \min\Bigg(\frac{f(x(n))}{x(n)}, \frac{\hat{f}\theta}{P_T - \theta y(n)} \Bigg) y(n) \Bigg\},
\end{aligned}
\tag{2.4}
$$

$$
y(n + 1) = y(n) \exp\Bigg\{ \min\Bigg\{ \hat{e}f(x(n)), \frac{P_T - \theta y(n)}{\theta} \frac{f(x(n))}{x(n)}, \frac{\hat{e}\hat{f}\theta x(n)}{P_T - \theta y(n)} \Bigg\} - d \Bigg\}
$$

for $n \in \mathbb{N}$.

In the following sections, we focus our attention on system (2.4). Throughout the rest of this paper, we consider only biologically meaningful initial values. Thus, we assume that $x(0) > 0$ and $P_T/\theta > y(0) > 0$. And it is easy to check that the solution S of system (2.4) is positive for all $n \in \mathbb{N}$.

3 Boundedness and invariance

In this section, we establish the following boundedness and positive invariant results for system (2.4) by carrying out arguments similar to those in Fan *et al.* [12].

For convenience, we assume that $f(x) = xp(x)$. In Loladze *et al.* [17], it has been proven that

$$
\lim_{x \to 0} p(x) = f'(0) < \infty, \qquad p'(x) < 0 \quad \text{for } x > 0.
$$

Theorem 3.1 *For system* (2.4), *we have, for all* $n \in \mathbb{N}^+$,

$$x(n) \leq \max\left\{x(0), \frac{K}{b}\exp(b-1)\right\} \equiv U,$$

$$y(n) \leq \max\{y(0), v\}\exp(2\hat{e}f(U)-2d) \equiv V,$$

where v *is any number satisfying* $\hat{e}f(U\exp(b-p(U)v)) < d$.

Proof By using the fact that $\max_{x\in\mathbb{R}} x\exp(b-\frac{bx}{K}) = \frac{K}{b}\exp(b-1)$ for $b > 0$, from system (2.4) we obtain

$$x(n+1) < x(n)\exp\left\{b - \frac{bx(n)}{K}\right\} \leq \frac{K}{b}\exp(b-1) \equiv u.$$

Hence, for all $n \in \mathbb{N}$, we have

$$x(n) \leq \max\{x(0), u\} \equiv U.$$

If $\hat{e}f(U) \leq d$, then it is clear that, for all $n \in \mathbb{N}^+$, we have $y(n) \leq y(0)$. We thus assume below that $\hat{e}f(U) > d$. Let v be large enough so that

$$\hat{e}f(U\exp(b-p(U)v)) < d.$$

We claim that for all $n \in \mathbb{N}$ we have

$$y(n) \leq \max\{y(0), v\}\exp(2\hat{e}f(U)-2d) \equiv V.$$

This is obviously true for $n = 1, 2$. In the following, we distinguish two cases to prove the claim.

Case 1. $y(0) \leq v$. If the claim is not true, then, for some $n_1 > 2$, $v < y(n_1 - 2) \leq V$, $v < y(n_1 - 1) \leq V$, and $y(n_1) > V$. In this case, using the assumption that $p'(x) < 0$, we have

$$x(n_1 - 1) \leq x(n_1 - 2)\exp(b - p(x(n_1 - 2))y(n_1 - 2)) < U\exp(b - p(U)v).$$

This implies that

$$y(n_1) < y(n_1 - 1)\exp\{\hat{e}f(U\exp(b-p(U)v)) - d\} < y(n_1 - 1) \leq V,$$

which contradicts $y(n_1) > V$.

Case 2. $y(0) > v$. In this case, we have $x(1) < U\exp(b - p(U)v)$, which implies that $y(2) < y(1)$. In other words, as long as $y(n) > v$, we have $y(n + 2) < y(n + 1)$. Hence there are two possibilities: either (i) for some $y(n^*) \leq v$ for some $n^* \in \mathbb{N}^+$; or (ii) $y(n) > v$ for all $n \in \mathbb{N}^+$. In case (ii), $y(n)$ is strictly decreasing for $n > 1$ and the claim is obviously true. In case (i), from the proof of case 1, we see that for $y(n) < V$ for $n > n^*$, and hence the claim is also true. This completes the proof. □

The positive invariance of

$$\Delta = \left\{ (x, y) : 0 < x < \frac{K}{b} \exp(b - 1), 0 < y < v \right\}$$

is a straightforward consequence of the above theorem.

Theorem 3.2 *For system* (2.4), Δ *is globally attractive with respect to the initial values* $(x(0), y(0))$ *such that* $x(0) > 0$ *and* $P_T/\theta > y(0) > 0$.

Proof In view of Theorem 3.1, it is easy to see that Δ is a positively invariant domain of system (2.4) and for large values of n, $x(n) \in (0, \frac{K}{b} \exp(b-1))$. Notice that if $y(n) > v$ for large values of $n \in \mathbb{N}^+$, then $y(n)$ must have $y^* = \limsup_{x \to \infty} y(n) \geq v$ by boundedness. Hence, for large values of n, we have

$$y(n) < y(n - 1) \exp\{\hat{e}f(U \exp(b - p(U)v)) - d\}.$$

Letting $n \to \infty$ yields

$$y^* \leq y^* \exp\{\hat{e}f(U \exp(b - p(U)v)) - d\} < y^*.$$

This contradicts $y^* > v > 0$. Then, for large values of n, $y(n) \in (0, v)$, proving the theorem. $\square$

4 Nullclines

In this section, we focus on analyzing the stability of the equilibria of (2.4). For convenience, we rewrite equation (2.4) as

$$
\begin{aligned}
x(n + 1) &= x(n) \exp\{F(x(n), y(n))\}, \\
y(n + 1) &= y(n) \exp\{G(x(n), y(n))\},
\end{aligned}
\tag{4.1}
$$

where

$$F(x, y) = b - \frac{bx}{\min\{K, (P_T - \theta y)/q\}} - \min\left\{ p(x), \frac{\hat{f}\theta}{P_T - \theta y} \right\} y,$$

$$G(x, y) = \min\left\{ \hat{e}xp(x), \frac{P_T - \theta y}{\theta} p(x), \frac{\hat{e}\hat{f}\theta x}{P_T - \theta y} \right\} - d.$$

To find the equilibrium points of equation (2.4), we solve

Producer nullclines: $x[1 - \exp\{F(x, y)\}] = 0$,   i.e., $x = 0$ or $F(x, y) = 0$,

Grazer nullclines: $y[1 - \exp\{G(x, y)\}] = 0$,   i.e., $y = 0$ or $G(x, y) = 0$.

The Jacobian of (2.4) is

$$J(x, y) = \begin{pmatrix} \exp\{F(x, y)\} + x \exp\{F(x, y)\}F_x(x, y) & x \exp\{F(x, y)\}F_y(x, y) \\ y \exp\{G(x, y)\}G_x(x, y) & \exp\{G(x, y)\} + y \exp\{G(x, y)\}G_y(x, y) \end{pmatrix},$$

$$\tag{4.2}$$

where

$$F_x(x,y) = \frac{\partial F(x,y)}{\partial x} = \begin{cases} -\frac{b}{\min\{K,\frac{P_T-\theta y}{q}\}} - p'(x)y, & \text{if } f(x) < \frac{\hat{f}\theta}{Q}, \\ -\frac{b}{\min\{K,\frac{P_T-\theta y}{q}\}} < 0, & \text{if } f(x) > \frac{\hat{f}\theta}{Q}, \end{cases}$$

$$F_y(x,y) = \frac{\partial F(x,y)}{\partial y} = \begin{cases} -p(x) < 0, & \text{if } f(x) < \frac{\hat{f}\theta}{Q}, K < \frac{P_T-\theta y}{q}, \\ -\frac{P_T\hat{f}\theta}{(P_T-\theta y)^2} < 0, & \text{if } f(x) > \frac{\hat{f}\theta}{Q}, K < \frac{P_T-\theta y}{q}, \\ -\frac{bq\theta x}{(P_T-\theta y)^2} - p(x) < 0, & \text{if } f(x) < \frac{\hat{f}\theta}{Q}, K > \frac{P_T-\theta y}{q}, \\ -\frac{bq\theta x}{(P_T-\theta y)^2} - \frac{P_T\hat{f}\theta}{(P_T-\theta y)^2} < 0, & \text{if } f(x) > \frac{\hat{f}\theta}{Q}, K > \frac{P_T-\theta y}{q}, \end{cases} \tag{4.3}$$

$$G_x(x,y) = \frac{\partial G(x,y)}{\partial x} = \begin{cases} \hat{e}[p(x) + xp'(x)] > 0, & \text{if } \hat{e}f(x) < \frac{Q}{\theta}f(x), \hat{e}f(x) < \hat{e}\hat{f}\frac{\theta}{Q}, \\ \frac{P_T-\theta y}{\theta}p'(x) < 0, & \text{if } \frac{Q}{\theta}f(x) < \hat{e}f(x), \frac{Q}{\theta}f(x) < \hat{e}\hat{f}\frac{\theta}{Q}, \\ \frac{\hat{e}\hat{f}\theta}{P_T-\theta y} > 0, & \text{if } \hat{e}\hat{f}\frac{\theta}{Q} < \hat{e}f(x), \hat{e}\hat{f}\frac{\theta}{Q} < \frac{Q}{\theta}f(x), \end{cases}$$

$$G_y(x,y) = \frac{\partial G(x,y)}{\partial y} = \begin{cases} 0, & \text{if } \hat{e}f(x) < \frac{Q}{\theta}f(x), \hat{e}f(x) < \hat{e}\hat{f}\frac{\theta}{Q}, \\ -p(x) < 0, & \text{if } \frac{Q}{\theta}f(x) < \hat{e}f(x), \frac{Q}{\theta}f(x) < \hat{e}\hat{f}\frac{\theta}{Q}, \\ \frac{\hat{e}\hat{f}\theta^2 x}{(P_T-\theta y)^2} > 0, & \text{if } \hat{e}\hat{f}\frac{\theta}{Q} < \hat{e}f(x), \hat{e}\hat{f}\frac{\theta}{Q} < \frac{Q}{\theta}f(x). \end{cases}$$

4.1 Boundary equilibria

We use the following standard lemma (see Edelstein-Keshet [9], p. 57) to study the stability of equilibrium points of system (2.4).

Lemma 4.1 (Jury test) *Let A be a 2×2 constant matrix. Both characteristic roots of A have magnitude less than 1 if and only if*

$$2 > 1 + \text{Det}(A) > \big|\text{Tr}(A)\big|. \tag{4.4}$$

In order to find the possible equilibrium points of system (2.4), we solve the equations

$$x\big[1 - \exp\{F(x,y)\}\big] = 0, \qquad y\big[1 - \exp\{G(x,y)\}\big] = 0.$$

It is easy to see that the equilibria of equation (2.4) are exactly the same as those of equation (2.1). The only boundary equilibrium points are $E_0 = (0,0)$ and $E_1 = (k,0)$.

The Jacobian matrix (4.2) at the origin E_0 turns out to be

$$J(E_0) = \begin{pmatrix} e^b & 0 \\ 0 & e^{-d} \end{pmatrix}.$$

It is clear that the magnitude of characteristic root e^{-d} is less than 1 while the magnitude of e^b is larger than 1. Consequently, E_0 is always unstable.

The Jacobian matrix (4.2) at E_1 becomes

$$J(E_1) = \begin{pmatrix} 1 - b & kF_y(k,0) \\ 0 & \exp\{G(k,0)\} \end{pmatrix},$$

where

$$G(k,0) = \min\left\{\hat{e}kp(k), \frac{P_T}{\theta}p(k), \frac{\hat{e}\hat{f}\theta k}{P_T}\right\} - d.$$

From Lemma 4.1, we obtain the following theorem.

Theorem 4.1 *For* (2.4), E_0 *is always unstable.* E_1 *is locally asymptotically stable* (*LAS*) *if*

$$0 < b < 2 \quad and \quad \min\left\{\hat{e}kp(k), \frac{P_T}{k\theta}p(k), \frac{\hat{e}\hat{f}\theta k}{P_T}\right\} < d;$$

it is unstable if

$$b > 2 \quad or \quad \min\left\{\hat{e}kp(k), \frac{P_T}{k\theta}p(k), \frac{\hat{e}\hat{f}\theta k}{P_T}\right\} > d.$$

Proof If we let λ_1 and λ_2 be the characteristic roots of $J(E_1)$, then the condition

$$0 < b < 2 \quad and \quad \min\left\{\hat{e}kp(k), \frac{P_T}{k\theta}p(k), \frac{\hat{e}\hat{f}\theta k}{P_T}\right\} < d$$

ensures that $|\lambda_i| < 1$, $i = 1, 2$, while the condition

$$b > 2 \quad or \quad \min\left\{\hat{e}kp(k), \frac{P_T}{k\theta}p(k), \frac{\hat{e}\hat{f}\theta k}{P_T}\right\} < d$$

implies $|\lambda_1| > 1$ or $|\lambda_2| > 1$. □

4.2 Internal equilibria

From [21], we claim that equation (2.4) could have multiple interior equilibria because both equations (2.1) and (2.4) have the same equilibria. Now we assume that $E^*(x^*, y^*)$ is such an equilibrium and discuss its local stability.

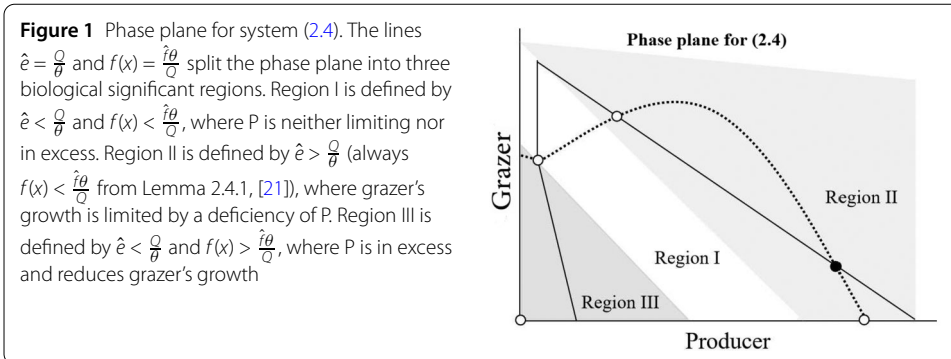The Jacobian (4.2) matrix at the positive equilibria E^* becomes

$$J(E^*) = \begin{pmatrix} 1 + x^*F_x & x^*F_y \\ y^*G_x & 1 + y^*G_y \end{pmatrix},$$

where

$$F_x = F_x(x^*, y^*), \qquad F_y = F_y(x^*, y^*), \quad G_x = G_x(x^*, y^*), \qquad G_y = G_y(x^*, y^*).$$

Its trace and determinant are

$$\mathrm{Tr}(J(E^*)) = 2 + x^*F_x + y^*G_y,$$
$$\mathrm{Det}(J(E^*)) = 1 + x^*F_x + y^*G_y + x^*y^*[F_xG_y - F_yG_x]$$
$$= \mathrm{Tr}(J(E^*)) - 1 + x^*y^*[F_xG_y - F_yG_x],$$

Figure 1 Phase plane for system (2.4). The lines $\hat{e} = \frac{Q}{\theta}$ and $f(x) = \frac{\hat{f}\theta}{Q}$ split the phase plane into three biological significant regions. Region I is defined by $\hat{e} < \frac{Q}{\theta}$ and $f(x) < \frac{\hat{f}\theta}{Q}$, where P is neither limiting nor in excess. Region II is defined by $\hat{e} > \frac{Q}{\theta}$ (always $f(x) < \frac{\hat{f}\theta}{Q}$ from Lemma 2.4.1, [21]), where grazer's growth is limited by a deficiency of P. Region III is defined by $\hat{e} < \frac{Q}{\theta}$ and $f(x) > \frac{\hat{f}\theta}{Q}$, where P is in excess and reduces grazer's growth

respectively. By referenced [21], the phase plane is divided into three biologically significant regions by the two lines $\hat{e} = \frac{Q}{\theta}$ and $f(x) = \frac{\hat{f}\theta}{Q}$ to investigate the interior equilibrium E^* (see Fig. 1). We have the following theorem on the local asymptotically stability of E^*.

Theorem 4.2 *In Region I (i.e., $\hat{e} < \frac{Q}{\theta}$ and $f(x) < \frac{\hat{f}\theta}{Q}$), the following are true*:

- *If the producer's nullcline is increasing at E^* (i.e., $F_x > 0$), then E^* is unstable.*
- *If the producer's nullcline is decreasing at E^* (i.e., $F_x < 0$), and*

$$\frac{1}{2}x^*y^*F_yG_x - 2 < x^*F_x < x^*y^*F_yG_x,$$

then E^* is LAS.

- *If the producer's nullcline is decreasing at E^* (i.e., $F_x < 0$), and*

$$F_x > y^*F_yG_x \quad or \quad x^*F_x < \frac{1}{2}x^*y^*F_yG_x - 2,$$

then E^* is unstable.

In Region II (i.e., $\hat{e} > \frac{Q}{\theta}$ and $f(x) < \frac{\hat{f}\theta}{Q}$), the following are true:

- *If the slope of the producer's nullcline at E^* is greater than the grazer's (i.e., $-G_x/G_y < -F_x/F_y$), then E^* is unstable.*
- *If the slope of the grazer's nullcline at E^* is greater than the producer's (i.e., $-G_x/G_y > -F_x/F_y$), and*

$$\frac{1}{2}x^*y^*[F_yG_x - F_xG_y] - 2 < x^*F_x + y^*G_y < x^*y^*[F_yG_x - F_xG_y],$$

then E^* is LAS.

- *If the slope of the grazer's nullcline at E^* is greater than the producer's (i.e., $-G_x/G_y > -F_x/F_y$), and*

$$x^*F_x + y^*G_y < \frac{1}{2}x^*y^*[F_yG_x - F_xG_y] - 2 \quad or$$

$$x^*F_x + y^*G_y > x^*y^*[F_yG_x - F_xG_y],$$

then E^* is unstable.

In Region III (i.e., $\hat{e} < \frac{Q}{\theta}$ and $f(x) > \frac{\hat{f}\theta}{Q}$), the following are true:

- *If the slope of the grazer's nullcline at E^* is greater than the producer's (i.e., $-G_x/G_y > -F_x/F_y$), then E^* is unstable.*

- *If the slope of the producer's nullcline at E^* is greater than the grazer's (i.e., $-G_x/G_y < -F_x/F_y$), and*

$$\frac{1}{2}x^*y^*[F_yG_x - F_xG_y] - 2 < x^*F_x + y^*G_y < x^*y^*[F_yG_x - F_xG_y], \qquad (4.5)$$

  then E_2 is LAS.
- *If the slope of the producer's nullcline at E^* is greater than the grazer's (i.e., $-G_x/G_y < -F_x/F_y$), and*

$$\begin{aligned} &x^*F_x + y^*G_y < \frac{1}{2}x^*y^*[F_yG_x - F_xG_y] - 2 \quad or \\ &x^*F_x + y^*G_y > x^*y^*[F_yG_x - F_xG_y], \end{aligned} \qquad (4.6)$$

  then E^* is unstable.

Proof The LAS of E^* in Region I and II is obtained by using the same arguments as those used in the proof of Theorem 4.2 in [12] where the interested reader can find all the details. Therefore, here we focus on the stability of E^* in Region III, $\hat{e} < \frac{Q}{\theta}$ and $f(x) > \frac{\hat{f}\theta}{Q}$. Suppose that E^* lies in Region III, then system (4.3) yields that at E^*, $F_x < 0$, $F_y < 0$, $G_x > 0$, and $G_y > 0$.

Note that

$$\mathrm{Det}\big(J\big(E^*\big)\big) = 1 + x^*F_x + y^*G_y + x^*y^*F_yG_y\left[-\frac{G_x}{G_y} - \left(\frac{F_x}{F_y}\right)\right].$$

If the slope of the grazer's nullcline at E^* is greater than the producer's, i.e., $-G_x/G_y > -F_x/F_y$, then $1 + \mathrm{Det}(J(E^*)) < \mathrm{Tr}(J(E^*))$, which implies that equation (4.4) does not hold. Hence, E^* is unstable. If the slope of the producer's nullcline at E^* is greater than the grazer's, then

$$-\frac{G_x}{G_y} < -\frac{F_x}{F_y} < 0.$$

If equation (4.5) holds, then one can easily show that system (4.4) holds. Consequently, E^* is stable. If equation (4.6) is valid, then E^* is unstable since equation (4.4) is not valid. □

5 Numerical simulations

In this section, we carry out systematic numerical simulations to verify and deepen our analytical findings and to compare them with those of the corresponding continuous system. Specifically, we investigate how the discretization impacts the modeling of the dynamic interaction between grazer and producer.

For simplicity, and without any loss of generality, we choose the Monod type function $f(x) = cx/(a + x)$ as the functional response of the grazer and on the assumption in the section (3), $p(x) = c/(a + x)$. In order to compare the dynamical behaviors of the discrete-time model (5.1) and continuous-time model (5.2), we carry out numerical simulations using the same parameters as in [21]. The parameter values are listed in Table 1. These values were also used by Loladze *et al.* [17] and chosen as biologically realistic values obtained

from Anderson [1] and Urabe and Sterner [26]. We will simulate the following producer-grazer systems:
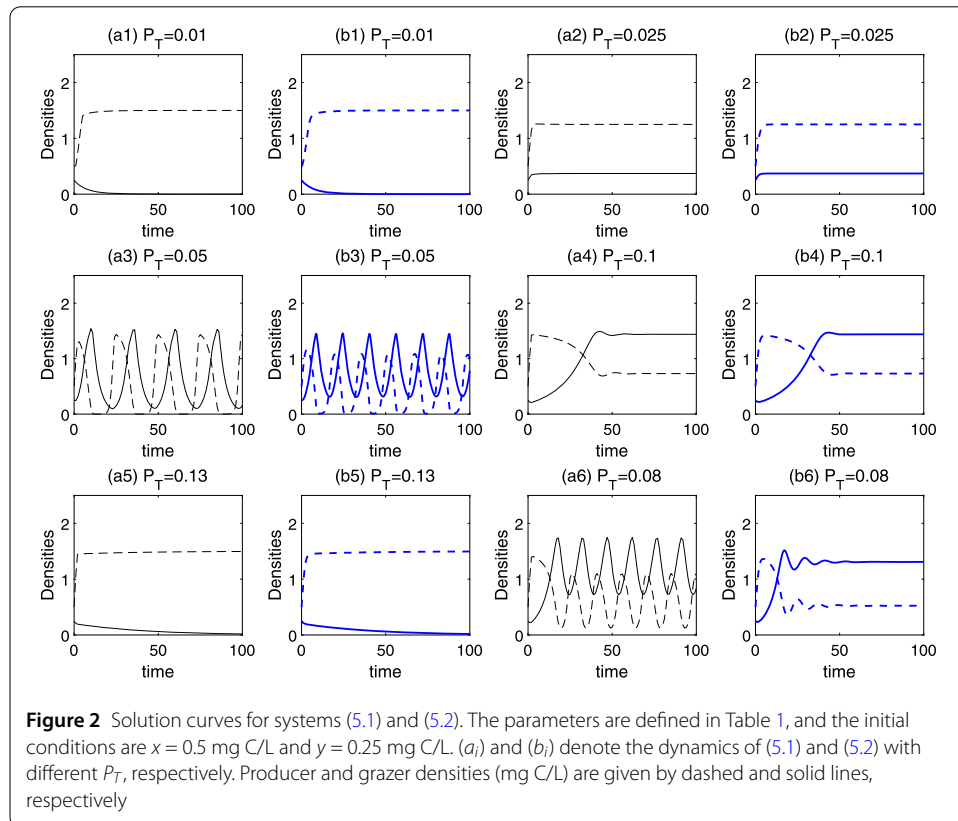
$$x(n + 1) = x(n) \exp\left\{ b - \frac{bx(n)}{\min\{K, (P_T - \theta y(n))/q\}} - \min\left\{ \frac{cy(n)}{a + x(n)}, \frac{\hat{f}\theta y(n)}{P_T - \theta y(n)} \right\} \right\},$$

$$y(n + 1) = y(n) \exp\left\{ \min\left\{ \hat{e}\frac{cx(n)}{a + x(n)}, \frac{P_T - \theta y(n)}{\theta x(n)}\frac{cx(n)}{a + x(n)}, \frac{\hat{e}\hat{f}\theta x(n)}{P_T - \theta y(n)} \right\} - d \right\}$$
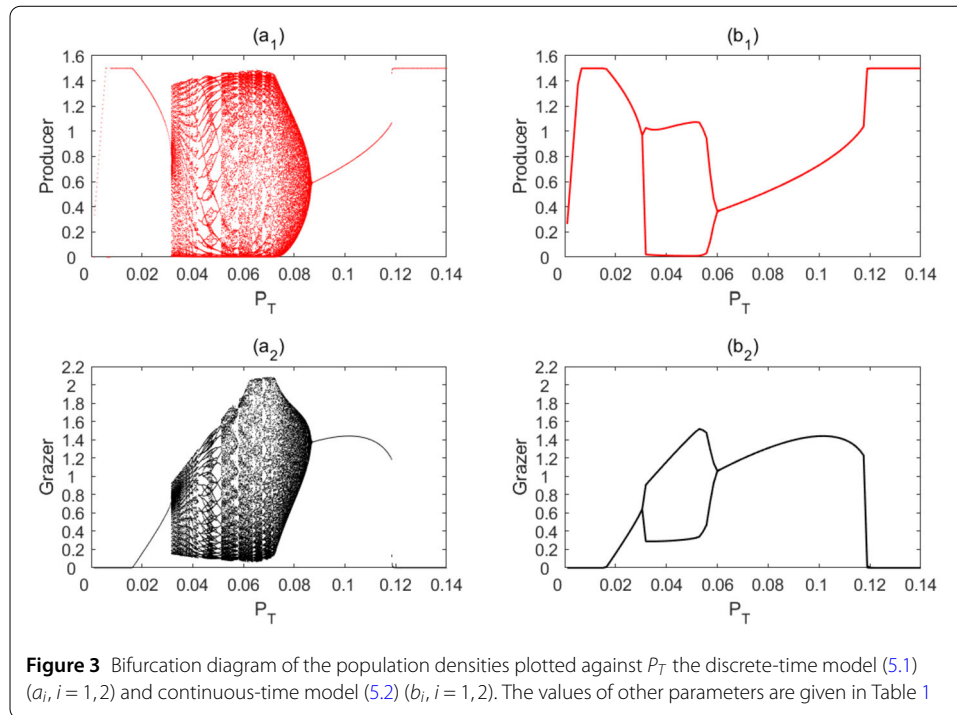
$$(5.1)$$

and

$$\frac{dx}{dt} = bx\left(1 - \frac{x}{\min\{K, (P_T - \theta y)/q\}} \right) - \min\left\{ \frac{cxy}{a + x}, \frac{\hat{f}\theta xy}{P_T - \theta y} \right\},$$

$$\frac{dy}{dt} = \min\left\{ \hat{e}\frac{cx}{a + x}, \frac{P_T - \theta y}{\theta x}\frac{cx}{a + x}, \frac{\hat{e}\hat{f}\theta x}{P_T - \theta y} \right\}y - dy.$$

$$(5.2)$$

In the numerical simulations, the initial values are set to $x(0) = 0.5$ mg C/L and $y(0) = 0.25$ mg C/L. The parameter P_T represents the total amount of P in the system. Since the producer takes up P, the P:C ratio of the producer is affected by the level of P. Low values of P will result in insufficient food nutrient content for the grazer, while high values of P will result in excess food nutrient content for the grazer.

In Fig. 2, we compare the solutions of the two systems with varying P_T. The dynamics of these two models are similar, but there are also some important differences between them. For very low values of P_T, the grazer cannot persist due to the very low food quan-
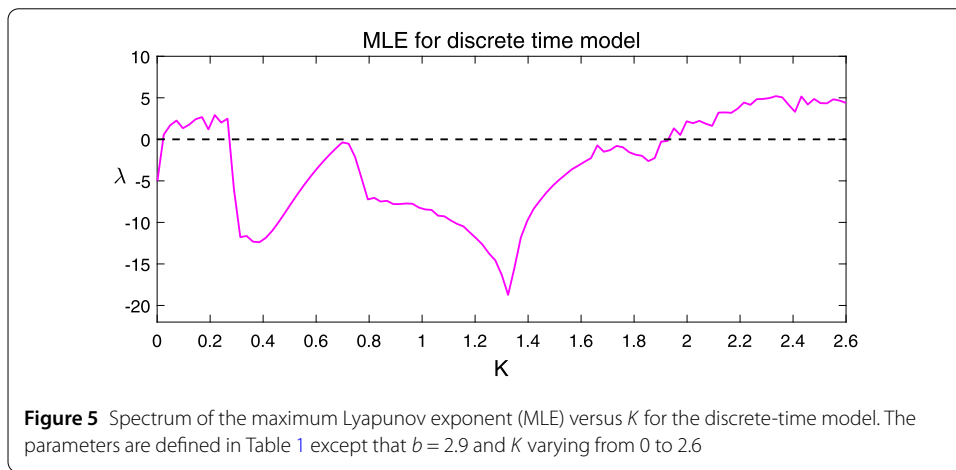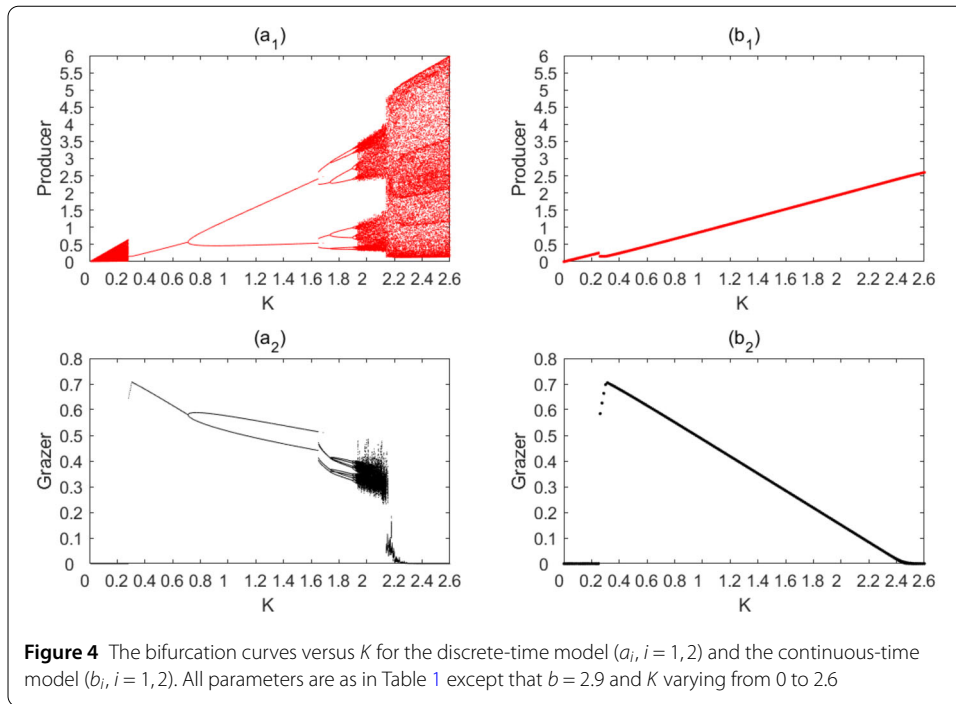

Figure 2 Solution curves for systems (5.1) and (5.2). The parameters are defined in Table 1, and the initial conditions are $x = 0.5$ mg C/L and $y = 0.25$ mg C/L. (a_i) and (b_i) denote the dynamics of (5.1) and (5.2) with different P_T, respectively. Producer and grazer densities (mg C/L) are given by dashed and solid lines, respectively

Figure 3 Bifurcation diagram of the population densities plotted against P_T the discrete-time model (5.1) ($a_i, i = 1, 2$) and continuous-time model (5.2) ($b_i, i = 1, 2$). The values of other parameters are given in Table 1

tity and starvation (see (a_1)–(b_1)). When P_T = 0.025 mg P/L, the population densities are at an equilibrium (see (a_2)–(b_2)). In both systems, we see periodic oscillations around an unstable equilibrium for P_T = 0.05 mg P/L (see (a_3)–(b_3)). However, in (a_3), we observe oscillations where grazer density reaches smaller values. When P_T = 0.08 mg P/L, (b_4) displays damped oscillations towards a stable equilibrium, whereas (a_4) shows periodic oscillations. When P_T = 0.1 mg P/L the oscillation disappears and equilibrium emerges (see (a_5)–(b_5)). For very high values of P_T, we see deterministic extinction caused by reduction of grazer growth due to high producer P:C or low food quality (see (a_6)–(b_6)).

The bifurcation diagrams in Fig. 3 illustrate how population dynamics in equations (5.1) and (5.2) vary with P_T. For P_T less than 0.015 mg P/L, the grazer cannot survive due to starvation. When P_T increases, the grazer persists at a stable equilibrium, and its density rises. When we increase P_T further, the system undergoes a Hopf bifurcation and the equilibrium loses its stability to a limit cycle, the amplitude of which increases with P_T. We can observe that the amplitude of the oscillation in the discrete model is larger than that in the continuous model. As P_T increases further, the limit cycle disappears through a saddle-node bifurcation and a new stable equilibrium appears. It can also be observed that the stable equilibrium of equation (5.2) emerges earlier than the corresponding one of equation (5.1). When we increase P_T still further, the grazer density begins to decline; although the producer density increases as P_T increases, its worsening quality significantly constrains the grazer's growth. For excess level of P_T, the grazer is heading toward deterministic extinction due to low food quality. Due to the extinction of grazer, the primary producer in both models tends to its carrying capacity. This type of scenario is often observed as phytoplankton blooms.

In fact, the discretization can have a significant impact on the dynamics of system (5.2). We further compare the dynamics of the continuous-time model (5.2) and the discrete-time model (5.1) by choosing the producer carrying capacity K as a bifurcation parameter.

Figure 4 The bifurcation curves versus K for the discrete-time model (a_i, $i = 1, 2$) and the continuous-time model (b_i, $i = 1, 2$). All parameters are as in Table 1 except that $b = 2.9$ and K varying from 0 to 2.6

Figure 5 Spectrum of the maximum Lyapunov exponent (MLE) versus K for the discrete-time model. The parameters are defined in Table 1 except that $b = 2.9$ and K varying from 0 to 2.6

There are some subtle differences between the dynamics of equations (5.1) and (5.2). From the bifurcation diagram in Fig. 4, we can easily observe that the dynamics of discrete-time model (5.1) are very different from those of the corresponding continuous-time model for $b = 2.9$ and K varying from 0 to 2.6. In continuous-time, the global attractor is either the boundary equilibrium or the internal equilibrium (see (b_1) and (b_2)), while in discrete-time, the global attractor can be a boundary equilibrium, internal equilibrium, limit cycles, or even a stranger attractor (chaos) (see (a_1) and (a_2)).

In Fig. 5, the existence interval of positive spectra of maximum Lyapunov exponent (MLE) of (5.1) proves that the discrete-time model exhibits chaos when K varies within the intervals (0.025, 0.28) and (1.95, 2.6). Figure 4(a_1) shows the familiar period-doubling route to chaos for the producer density. However, the grazer density crashes and instantly reaches zero immediately after the producer enters the chaotic zone (see Fig. 4(a_2)). This

suggests that chaotic behavior of the producer population provides an important factor for the extinction of grazer population. This interesting and important biological insight is totally lost in the continuous-time model (5.2) (see Fig. 4(b_1) and (b_2)). This also supports the point that the discretization can contribute to the occurrence of oscillation of the populations.

6 Conclusion and discussion

The theory of ecological stoichiometry has deepened our understanding of many ecological interactions [23]. Stoichiometry-based models provide more insight into population dynamics. Continuous-time models lead to several interesting results. An important question is how robust the model predictions are to time discretization. In this paper we develop and analyze a 2-D stoichiometric knife-edge discrete model. The model admits rich dynamics under the stoichiometric constraints.

Through the theoretical and numerical analysis, we find that many of the dynamical features exhibited by its continuous analogs (2.1) are captured in our discrete model (2.4). Indeed, the continuous and discrete stoichiometric models exhibit similar phenomena. The analysis presented here verifies that the effects of food quality and the resulting stoichiometric constraints on the grazer are qualitatively robust to discretization of time for certain parameter sets. In these stoichiometric models, the nutritional quality of the producer can lead to counterintuitive dramatic impacts on population dynamics. The notable point that high nutrient level can drive the grazer to deterministic extinction can also be observed in the discrete model.

It is important to note that for some particular parameter sets the two models predict qualitatively different dynamics. These differences are highlighted in the bifurcation diagrams for P_T (see Fig. 3). The amplitude of the cyclic oscillations of species in the discrete model is larger than that in the continuous model at the same fixed nutrient level, and they are presented at a larger range of parameter value P_T. These results highlight the fact that the discretization can make the system more prone to oscillation. Here, the dynamics of continuous system (2.1) can be significantly impacted by the discretization.

Additional differences between the two models are seen when K, the producer's carrying capacity, is chosen as the bifurcation parameter in Fig. 4. The bifurcation diagrams of both the discrete model (2.4) and the continuous model (2.1) show quite different dynamics with each other. The possible attractors of the continuous model (2.1) only include boundary equilibrium and internal equilibrium. However, the possible attractors of the discrete model (2.4) include boundary and internal equilibria, limit cycles, or even a strange attractor (chaos) (see Fig. 4). The positive maximum Lyapunov exponents of model (2.4) in some biologically reasonable region suggest that the discrete model exhibits chaotic dynamics. This result can also serve as a case study on the possibility of chaos in discrete stoichiometric systems [1, 12].

The stoichiometric features of the continuous model are robust to the time discretization, but the differences caused by discretization should not be neglected. Due to the importance and crucial implications of the time scaling in ecology, it is critical to select appropriate time scale in ecological modeling for a practical problem.

Competing interests
The authors declare that they have no competing interests.

Authors' contributions
All authors contributed equally to the manuscript and typed, read, and approved the final manuscript.

Author details
¹School of Science, Dalian Maritime University, Dalian, China. ²Department of Mathematics and Statistics, Texas Tech University, Lubbock, USA.

Publisher's Note
Springer Nature remains neutral with regard to jurisdictional claims in published maps and institutional affiliations.

References
1. Andersen, T.: Pelagic Nutrient Cycles: Herbivores as Sources and Sinks. Springer, Berlin (1997)
2. Asik, L., Kulik, J., Long, K., Peace, A.: Dynamics of a stoichiometric producer–grazer system with seasonal effects on light level. Math. Biosci. Eng. **16**, 501–515 (2018)
3. Asik, L., Peace, A.: Dynamics of a producer–grazer model incorporating the effects of phosphorus loading on grazer's growth. Bull. Math. Biol. **81**(5), 1352–1368 (2019)
4. Boersma, M., Elser, J.J.: Too much of a good thing: on stoichiometrically balanced diets and maximal growth. Ecology **87**, 1325–1330 (2006)
5. Busenberg, S., Cooke, K.L.: Models of vertically transmitted diseases with sequential-continuous dynamics. In: Nonlinear Phenomena in Mathematical Sciences, pp. 179–187 (1982)
6. Chen, M., Fan, M., Kuang, Y.: Global dynamics in a stoichiometric food chain model with two limiting nutrients. Math. Biosci. **289**, 9–19 (2017)
7. Chen, M., Fan, M., Xie, C.B., Peace, A., Wang, H.: Stoichiometric food chain model on discrete time scale. Math. Biosci. Eng. **16**, 101–118 (2019)
8. Cooke, K.L., Wiener, J.: Retarded differential equations with piecewise constant delays. J. Math. Anal. Appl. **99**, 265–297 (1984)
9. Edelstein-Keshet, L.: Mathematical Models in Biology (1988)
10. Elser, J.J., Loladze, I., Peace, A., Kuang, Y.: Lotka re-loaded: modeling trophic interactions under stoichiometric constraints. Ecol. Model. **245**, 3–11 (2012)
11. Elser, J.J., Watts, J., Schampel, J.H., Farmer, J.: Early Cambrian food webs on a trophic knife-edge? A hypothesis and preliminary data from a modern stromatolite-based ecosystem. Ecol. Lett. **9**(3), 295–303 (2006)
12. Fan, M., Loladze, I., Kuang, Y., Elser, J.J.: Dynamics of a stoichiometric discrete producer–grazer model. J. Differ. Equ. Appl. **11**, 347–364 (2005)
13. Frankham, R., Brook, B.W.: The importance of time scale in conservation biology and ecology. Ann. Zool. Fenn. **41**, 459–463 (2004)
14. Gurney, W., Nisbet, R.M.: Ecological Dynamics. Oxford University Press, Oxford (1998)
15. Kuang, Y., Huisman, J., Elser, J.J.: Stoichiometric plant–herbivore models and their interpretation. Math. Biosci. Eng. **1**, 215–222 (2004)
16. Li, W.T., Huo, H.F.: Positive periodic solutions of delay difference equations and applications in population dynamics. J. Comput. Appl. Math. **176**, 357–369 (2005)
17. Loladze, I., Kuang, Y., Elser, J.J.: Stoichiometry in producer–grazer systems: linking energy flow with element cycling. Bull. Math. Biol. **62**, 1137–1162 (2000)
18. Loladze, I., Kuang, Y., Elser, J.J., Fagan, W.F.: Competition and stoichiometry: coexistence of two predators on one prey. Theor. Popul. Biol. **65**, 1–15 (2004)
19. Peace, A.: Effects of light, nutrients, and food chain length on trophic efficiencies in simple stoichiometric aquatic food chain models. Ecol. Model. **312**, 125–135 (2015)
20. Peace, A., Wang, H., Kuang, Y.: Dynamics of a producer–grazer model incorporating the effects of excess food nutrient content on grazer's growth. Bull. Math. Biol. **76**, 2175–2197 (2014)
21. Peace, A., Zhao, Y., Loladze, I., Elser, J.J., Kuang, Y.: A stoichiometric producer–grazer model incorporating the effects of excess food-nutrient content on consumer dynamics. Math. Biosci. **244**, 107–115 (2013)
22. Saleem, M., Agrawal, T., Anees, A.: A study of tumour growth based on stoichiometric principles: a continuous model and its discrete analogue. J. Biol. Dyn. **8**, 117–134 (2014)
23. Sterner, R.W., Elser, J.J.: Ecological Stoichiometry: The Biology of Elements from Molecules to the Biosphere. Princeton University Press, Princeton (2002)
24. Sui, G., Fan, M., Loladze, I., et al.: The dynamics of a stoichiometric plant–herbivore model and its discrete analog. Math. Biosci. Eng. **4**(1), 29–46 (2007)
25. Turchin, P.: Complex Population Dynamics: A Theoretical/Empirical Synthesis. Monographs in Population Biology, vol. 35. Princeton University Press, Princeton (2003)
26. Urabe, J., Sterner, R.W.: Regulation of herbivore growth by the balance of light and nutrients. Proc. Natl. Acad. Sci. USA **93**, 8465–8469 (1996)

27. Wang, H., Kuang, Y., Loladze, I.: Dynamics of a mechanistically derived stoichiometric producer–grazer model. J. Biol. Dyn. **2**, 286–296 (2008)

28. Xie, C., Fan, M., Zhao, W.: Dynamics of a discrete stoichiometric two predators one prey model. J. Biol. Syst. **18**, 649–667 (2010)